

Cite this: *Chem. Sci.*, 2025, 16, 22588

All publication charges for this article have been paid for by the Royal Society of Chemistry

# A proto-aldehyde fluorescence quenched substrate for quantitative imaging of both protein and enzyme activity within cells†

Sha Zhu,<sup>‡a</sup> Matthew C. Deen,<sup>‡a</sup> Samy Cecioni,<sup>§a</sup> Kim Lam Wong,<sup>b</sup> Evan Perley-Roberston,<sup>a</sup> Weifeng Benny Wu<sup>a</sup> and David J. Vocadlo<sup>\*,ab</sup>

Fluorogenic substrates are emerging tools that enable studying enzymatic processes within their native cellular environments. However, fluorogenic substrates that function within live cells are generally incompatible with cellular fixation, preventing their tandem application with fundamental cell biology methods such as immunocytochemistry. Here we report a simple approach to enable the stable chemical fixation of the fluorescent product of a series of dark-to-light bis-acetal based substrates (BABS). Cleavage of the BABS glycosidic bond leads to liberation of a hemiacetal in which one branch consists of a proto-aldehyde bearing the fluorophore and the other branch consists of an alcohol bearing the quencher. Spontaneous breakdown of this hemiacetal leads to formation of a fluorescent aldehyde. Trapping of this aldehyde by standard reductive amination to intracellular proteins allows its stable retention within cells and concomitant imaging of cellular proteins by traditional immunocytochemistry. These bis-acetal substrates enable measuring changes in lysosomal GCase activity in response to both chemical and genetic perturbations. These tools will aid in studying the role of GCase activity in diseases and accelerate the creation of new therapeutic approaches targeting the GCase pathway. We also expect this strategy to be broadly useful for creating fixable substrates for other lysosomal enzymes.

Received 25th June 2025  
Accepted 7th October 2025

DOI: 10.1039/d5sc04671h

rsc.li/chemical-science

## Introduction

An increasing body of research on fluorescence-quenched substrates holds promise for developing new approaches to studying cellular processes that regulate various disease-associated enzymes. By leveraging bright fluorophores and efficient fluorescence quenchers, these chemical tools undergo highly sensitive dark-to-light transitions that enable quantifying enzymatic activity within live cells.<sup>1</sup> A common limitation associated with the use of such fluorescence-quenched substrates is that they can only be used to report on enzymatic activity and cannot be used in conjunction with a range of other strategies that permit concomitant imaging of biomolecules. Nevertheless, their application in studying the effects of either genetic or small molecule perturbations would be

enhanced by the ability to combine activity measurements with simultaneous observation of disease-associated proteins, subcellular markers, RNA and other biomolecules.<sup>2–4</sup> Being able to reliably perform such studies would allow for simple direct cellular correlations between activity measurements and the presence, localization, and levels not only of such enzymes but also of various cellular factors that can modify their activities. Various efforts have been made to address this need, including for the family of glycoside hydrolases, the creation of simply poly-lysine derivatives that can be “fixed” within cells using standard cell biological methods.<sup>5</sup> However, this approach necessitates chemical modification of the substrate carbohydrate moiety at two separate locations, which is not tolerated by some enzymes.

We envisioned one approach to address this shortcoming that advances the concept of bis-acetal-based substrates (BABS).<sup>6,7</sup> These substrates undergo a dark-to-light transition upon enzymatic hydrolysis of the glycosidic bond by releasing an aglycone comprising a hemiacetal. This hemiacetal then spontaneously decomposes to yield an aldehyde fragment and an alcohol fragment that physically separate by diffusion to relieve quenching and unmask fluorescence in an enzyme dependent manner. Notably, this strategy avoids the need to modify the carbohydrate moiety of the substrate, making the approach general to glycoside hydrolases. Here, we

<sup>a</sup>Department of Chemistry, Simon Fraser University, Burnaby, BC V5A 1S6, Canada.  
E-mail: dvocadlo@sfu.ca

<sup>b</sup>Department of Molecular Biology and Biochemistry, Burnaby, BC V5A 1S6, Canada

† The term proto-aldehyde is used to convey that the substrate, which contains two arms, contains an aldehyde that is only exposed after enzymatic cleavage of the glycosidic bond and spontaneous breakdown.

‡ These authors contributed equally.

§ Current address: Department of Chemistry, Université de Montréal, Québec, Canada.

hypothesized that by positioning the fluorophore on the proto-aldehyde arm of the aglycone, the resulting fluorescent product would form imine adducts with lysine residues of intracellular proteins (Fig. 1A). Due to the covalent nature of this adduct and its reversibility in an aqueous solution, we anticipated such imine adducts could be made more stable by incorporating a reductive amination step using common hydride reagents. Such reagents, which are often used during imaging of tissue sections to reduce background fluorescence,<sup>8</sup> would result in conversion of these imine linkages to produce more stable secondary amine functionalities. As a model enzyme system to investigate this concept, we selected the lysosomal  $\beta$ -glucosidase, glucocerebrosidase (GCase, CAZY family GH30). Our choice was motivated by GCase activity being linked to several human diseases.<sup>9</sup> Bi-allelic loss-of-function mutations in *GBA1*, the gene encoding GCase, result in the development of Gaucher's disease (GD), a lysosomal storage disease caused by the accumulation of its substrate glucosylceramide.<sup>10</sup>

In addition to its involvement in GD, mono-allelic loss-of-function mutations in *GBA1* have been recently identified as the most prevalent genetic risk factor for the development of Parkinson's disease (PD).<sup>11</sup> Moreover, *GBA1*-associated PD patients suffer from earlier disease onset and a more severe form of the disease, suggesting an important role for GCase in the etiology of PD.<sup>12</sup> The variable penetrance of *GBA1* mutations in both of these diseases has stimulated the search for genetic modifiers of lysosomal GCase activity.

One approach that has been taken to understand this relationship is to identify pathways associated with pathogenesis

through the identification of genetic modifiers of penetrance of *GBA1* mutations in PD patients.<sup>13,14</sup> Nevertheless, few genes have been identified and the mechanisms by which the genes that have been found to influence GCase activity are not well understood.

Given the involvement of GCase in both GD and PD, and the high interest in GCase function and regulation, we envisioned that a simple-to-use fluorogenic GCase substrate that could be used both in living cells and fixed would be of value for studying this enzyme (Fig. 1B). Here we report the design and synthesis of a series of GCase targeted bis-acetal based substrates (BABS). We describe simple methods to fix the fluorescent product of GlcBABS that exploits existing and widely used cell biological approaches to show that optimized GlcBABS reports on the lysosomal activity of GCase quantitatively and selectively within both live and fixed cells. We illustrate the utility of BABS substrates by demonstrating that activity measurements can be performed in tandem with immunocytochemistry (ICC).

## Results and discussion

As this work is focused on identifying a GCase substrate that could be conveniently fixed and used to quantitatively image GCase activity along with lysosomal proteins by immunocytochemistry, we would address this need by taking advantage of recently developed bis-acetal-based substrates (BABS) for glycosidases<sup>6,7</sup> (Fig. 1A) as potential fixable substrates.

As a first step to test the feasibility of creating BABS substrates for monitoring GCase activity within both live and

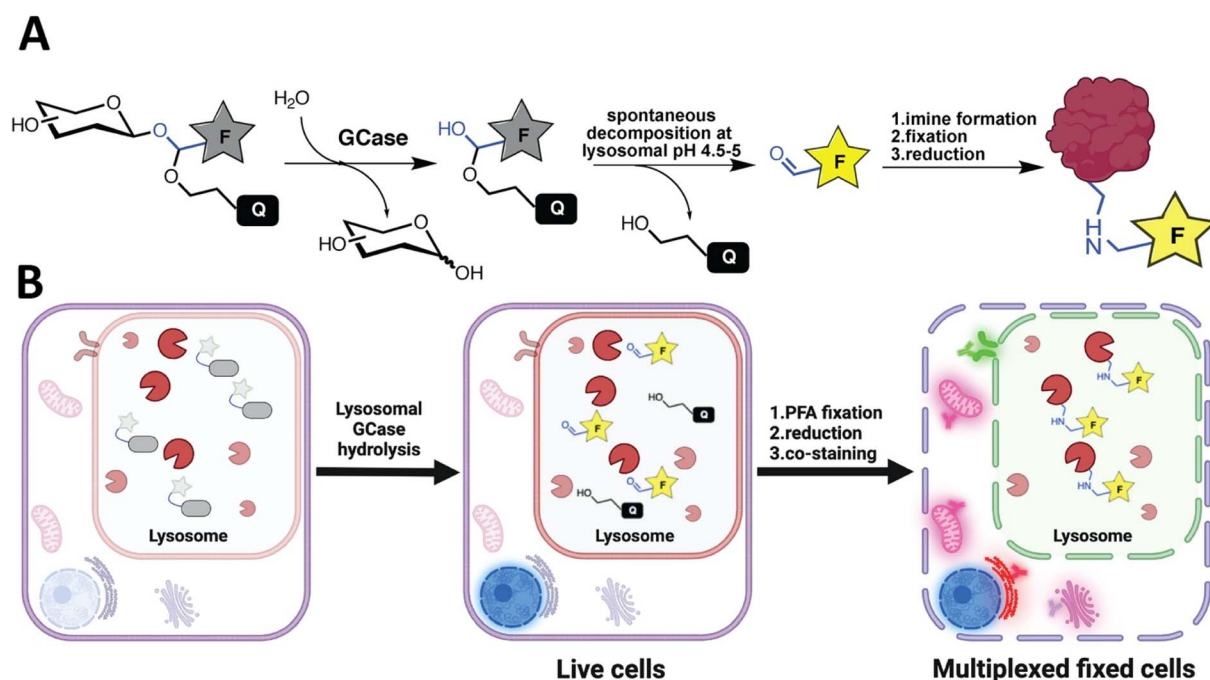


**Fig. 1** Mechanism of fluorogenesis for GlcBABS and intracellular imine labelling. (A) GCase-catalyzed cleavage of GlcBABS substrates leads to the release of a hemiacetal product which spontaneously decomposes, resulting in fluorescence signal release. The aldehyde-labelled fluorophores rapidly form transient imines with lysine residues of proteins. These imines can be trapped by chemical reduction with sodium cyanoborohydride. (B) Illustration of how GlcBABS could be used in both live and fixed cells to quantify GCase activity and, within fixed cells, concomitantly image other proteins and organelles by traditional immunocytochemistry.



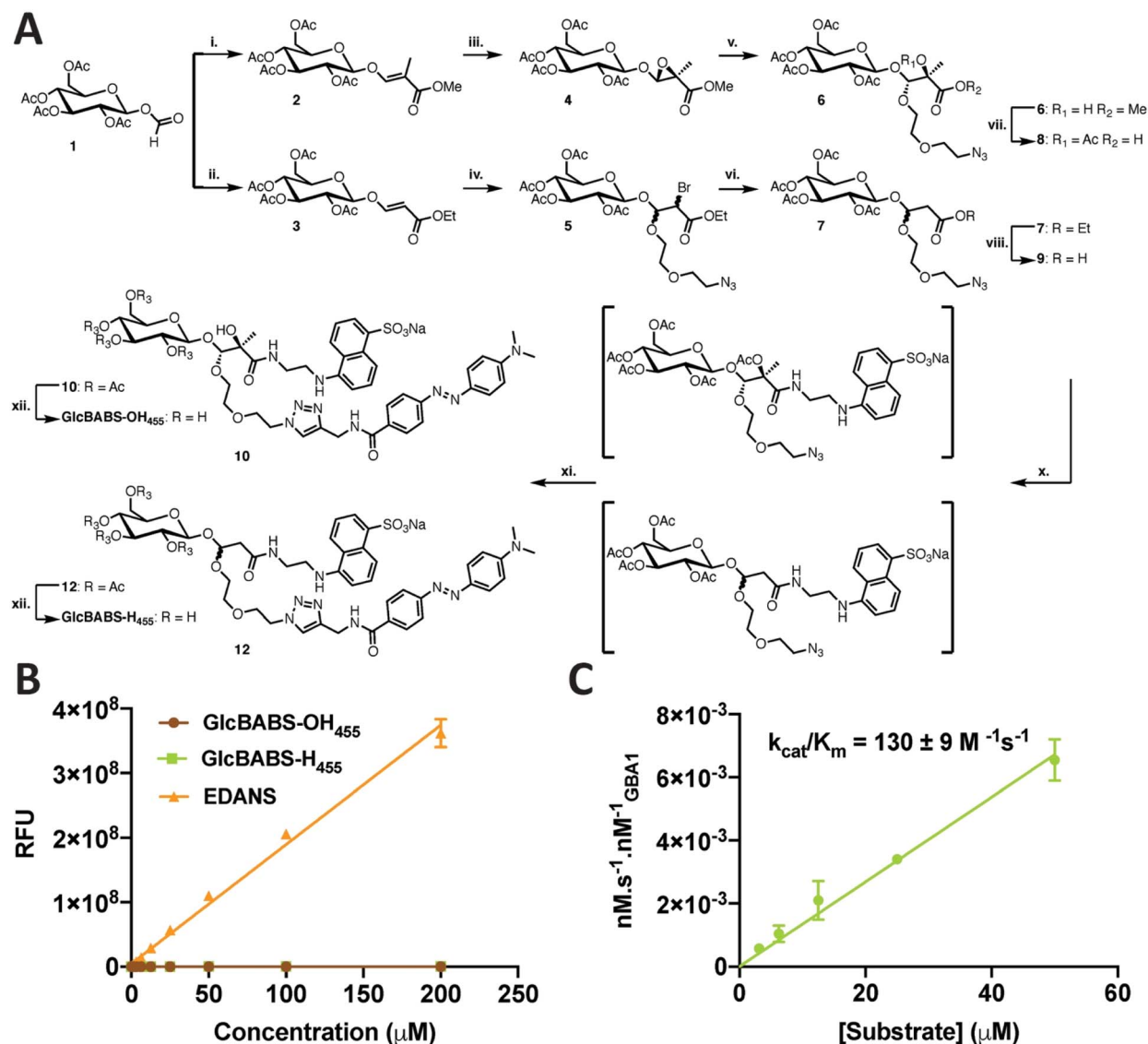


**Fig. 2** Synthesis of GlcBABS-OH<sub>455</sub> and GlcBABS-H<sub>455</sub>, the first and second generation GlcBABS substrates. (A) Synthetic route for GlcBABS-OH<sub>455</sub> and GlcBABS-H<sub>455</sub>. (i) (1) (2-Ethoxy-1-methyl-2-oxoethyl) tributyl phosphonium bromide (2.5 eq.), DCM; Aq. NaOH (10%) (2) toluene 110 °C; (ii) (1) ethoxycarbonylmethyl(triphenyl)phosphonium bromide (3 eq.), DCM; Aq. NaOH (10%), (2) toluene, 60 °C; (iii) mCPBA (1.4 eq.), toluene, 0 °C; (iv) (1) H-(OCH<sub>2</sub>CH<sub>2</sub>)<sub>2</sub>-N<sub>3</sub>, H<sub>2</sub>SO<sub>4</sub> (Cat.), NBS (1.2 eq.), DCM, 0 °C, (2) AIBN (0.2 eq.), NaBH<sub>3</sub>CN (2.5 eq.), Bu<sub>3</sub>SnCl (0.2 eq.), *t*-BuOH; (v) CSA (0.3 eq.) H-(OCH<sub>2</sub>CH<sub>2</sub>)<sub>2</sub>-N<sub>3</sub>, DCM; (vi) AIBN (0.2 eq.), NaBH<sub>3</sub>CN (2.5 eq.), Bu<sub>3</sub>SnCl (0.2 eq.), *t*-BuOH; (vii) (1) LiOH (10 eq.), THF, H<sub>2</sub>O, (2) pyridine, Ac<sub>2</sub>O; (viii) LiOH (10 eq.), THF, H<sub>2</sub>O (x) EDANS-NH<sub>2</sub> (1.2 eq.), DIPEA (4 eq.), HBTU (1.1 eq.), DMF; (xi) DABCYL alkyne (2.2 eq.), DIPEA (4 eq.), [Cu(CH<sub>3</sub>CN)<sub>4</sub>]PF<sub>6</sub> (0.3 eq.), DCM; (xii) NaOMe (7 eq.), MeOH. (B) Determination of fluorescence quenching efficiency through comparison of concentration dependence fluorescence intensity of each of EDANS and GlcBABS-H<sub>455</sub>. Error bars represent standard deviations ( $n = 3$ ). (C) Michaelis-Menten kinetics of GlcBABS-H<sub>455</sub> with recombinant GCase (rhGCase).

fixed cells, we designed a  $\beta$ -glucoside BABS (GlcBABS) substrate that could be tested *in vitro* to establish how efficiently this enzyme would process such a substrate. For simplicity, we incorporated an EDANS fluorophore on the proto-aldehyde arm of the hemiacetal product and a DABCYL quencher on the proto-alcohol arm. The synthesis started from penta-O-acetyl- $\alpha$ -D-glucosyl formate. Wittig olefination delivered the known vinyl glucoside **2**.<sup>15</sup> Epoxidation of the olefin using mCPBA afforded **4** in fair yield as a single diastereomer. This diastereomeric selectivity aligns with previous observations showing tetra-O-acetyl glucosides work well as chiral auxiliaries to induce

stereoselectivity in hydrogenation reactions.<sup>15</sup> Opening of the epoxide under acidic conditions using camphor sulfonic acid in the presence of 2-(2-azidoethoxy)ethan-1-ol enabled installation of both the bis-acetal motif as well as the azide functionality that could be later exploited as an orthogonal group for downstream functionalization. Hydrolysis of the ester groups followed by acetylation of the free alcohols afforded access to our desired bifunctional intermediate **8** bearing a carboxylic acid and an azide group to which we could couple our fluorophore and quencher pair. Using these orthogonal functional groups, we used successive amide coupling and copper-catalyzed azide-

alkyne cycloaddition (CuAAC) reactions to install the EDANS fluorophore ( $\lambda_{\text{ex,max}} = 336 \text{ nm}$ ,  $\lambda_{\text{em,max}} = 455 \text{ nm}$ ) and DABCYL ( $\lambda_{\text{abs,max}} = 479 \text{ nm}$ ) fluorescence quencher to obtain **10**, which was efficiently de-*O*-acetylated to obtain our target GlcBABS substrate GlcBABS-OH<sub>455</sub>. However, upon testing this material as a substrate of recombinant human GCase (rhGCase) we observed no turnover. This observation was surprising given that the glucose recognition motif is unmodified and also because other BABS substrates have been shown to be efficient substrates for other glycoside hydrolases.<sup>16</sup> We hypothesized that the relatively bulky quaternary center within the aglycone, which is proximal to the glycosidic oxygen, may not be tolerated within the active site of GCase.

To test this possibility, we set out to prepare a modified GlcBABS substrate in which the quaternary center was replaced by a methylene unit (GlcBABS-H<sub>455</sub>) (Fig. 2A). Starting from the same formyl glycoside **1**, Wittig-like olefination reaction was used to generate vinyl  $\beta$ -glucoside **3** lacking the methyl group positioned alpha to the carbonyl. To remove the alcohol present in GlcBABS-OH<sub>455</sub>, we avoided the epoxide intermediate by using bromoalkoxylation to create the bis-acetal functionality.<sup>6,17</sup> In contrast to the epoxidation reaction, this bromination reaction generated a mixture of diastereomers. To generate the desired methylene unit, the crude bromide was subjected to reductive debromination using *in situ* formed tributyltin hydride, affording the desired intermediate **7** in good yield. Protecting group manipulation of **7** yielded the desired bi-functionalized intermediate **9**. Sequential amide coupling and CuAAC reactions were used to sequentially install the EDANS and DABCYL fluorophore and quencher pair to obtain the per-*O*-acetylated substrate precursor **12**, in which the fluorophore is linked to the proto-aldehyde arm of the conjugate. This

penultimate product was efficiently deprotected using catalytic sodium methoxide to yield GlcBABS-H<sub>455</sub>. This route, which follows from our previous work on galacto-configured substrates, proved reliable and suggests its amenability to the production of differently configured monosaccharide-containing substrates.

With this material in hand, we were pleased to observe that GlcBABS-H<sub>455</sub> had an excellent quenching efficiency of >99.5% (Fig. 2B and C) and that incubation with rhGCase resulted in its efficient hydrolysis with a second-order rate constant ( $k_{\text{cat}}/K_{\text{m}} = 130 \pm 9 \text{ M}^{-1} \text{ s}^{-1}$ ) (Fig. 2C), which is comparable to that of other reported live cell substrates.<sup>5,18</sup> Furthermore, we assessed its selectivity for GCase relative to the other human  $\beta$ -glucosidases GBA2 and GBA3. We found that while GlcBABS-H<sub>455</sub> was hydrolyzed efficiently by GCase, we were unable to observe its turnover by GBA2 or GBA3 at enzyme concentrations up to 20 nM, suggesting cellular assays would show exceptional selectivity for GCase (Fig. S1). Taken together, the *in vitro* measurements of selectivity and sensitivity of the “decongested” GlcBABS-H<sub>455</sub> support this approach as suitable for delivering fluorogenic substrates to image GCase activity within cells.

Given the promising results we obtained with GlcBABS-H<sub>455</sub>, we next generated a derivative for live cell experiments. To reduce background arising from cellular autofluorescence, we took advantage of the ability to perform late-stage derivatization and exchanged the blue-shifted EDANS for the more red-shifted TAMRA. After preparing the TAMRA-bearing derivative GlcBABS-H<sub>563</sub> (Fig. 3A), we measured its quenching efficiency to be >99.4% and its second order rate constant for turnover by GCase ( $k_{\text{cat}}/K_{\text{M}} = 3400 \pm 547 \text{ M}^{-1} \text{ s}^{-1}$ , Fig. S2). These favourable properties support the suitability of GlcBABS-H<sub>563</sub> for live cell

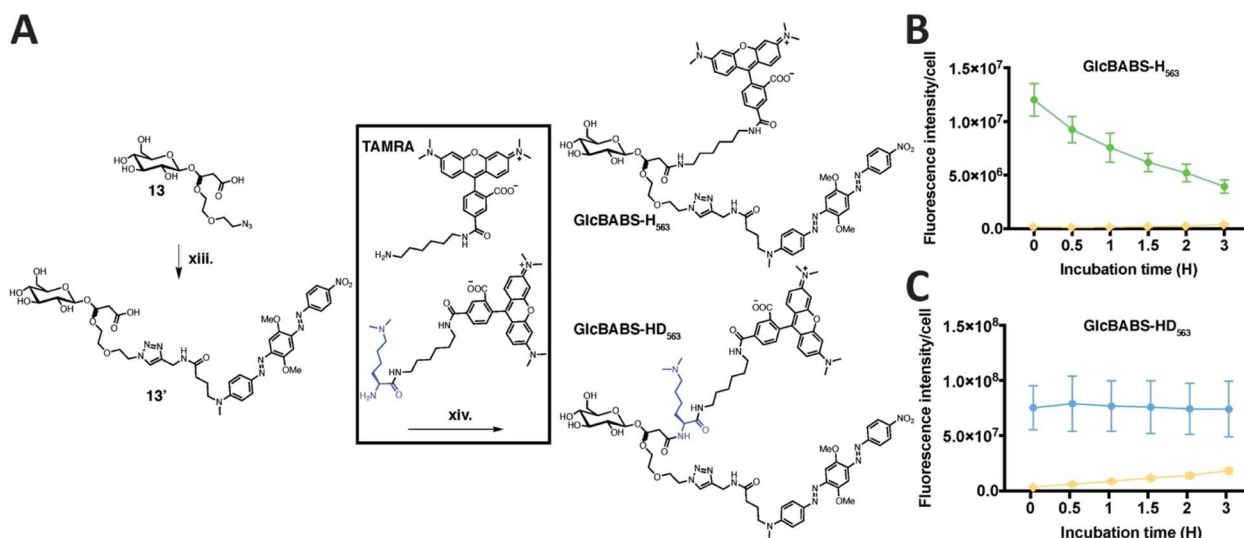


**Fig. 3** Investigation of the effects of the dML moiety on the cellular retention and stability of the fluorescence signal arising from GCase catalyzed hydrolysis of GlcBABS substrates. (A) Synthesis of GlcBABS-H<sub>563</sub> and GlcBABS-HD<sub>563</sub>. (xiii) BHQ-2 alkyne (1.2 eq.), Cu(II)SO<sub>4</sub> (0.5 eq.), sodium ascorbate (0.5 eq.), BTAA (0.1 eq.), DMF : H<sub>2</sub>O : MeOH : DCM (2 : 1 : 1 : 1). (xiv) TAMRA-NH<sub>2</sub> (1.2 eq.), DIPEA (4 eq.), HBTU (1.1 eq.), DMF. (B) Quantification of fluorescent signal loss of GlcBABS-H<sub>563</sub> in SK-N-SH cells. WT cells incubated with GlcBABS-H<sub>563</sub> and with (yellow) or without (green) inhibitor AT3375. (C) Quantification of fluorescent signal loss of GlcBABS-HD<sub>563</sub> in SK-N-SH cells. WT cells incubated with GlcBABS-HD<sub>563</sub> and with (yellow) or without (blue) inhibitor AT3375. Error bars represent SEM over 3 replicates.



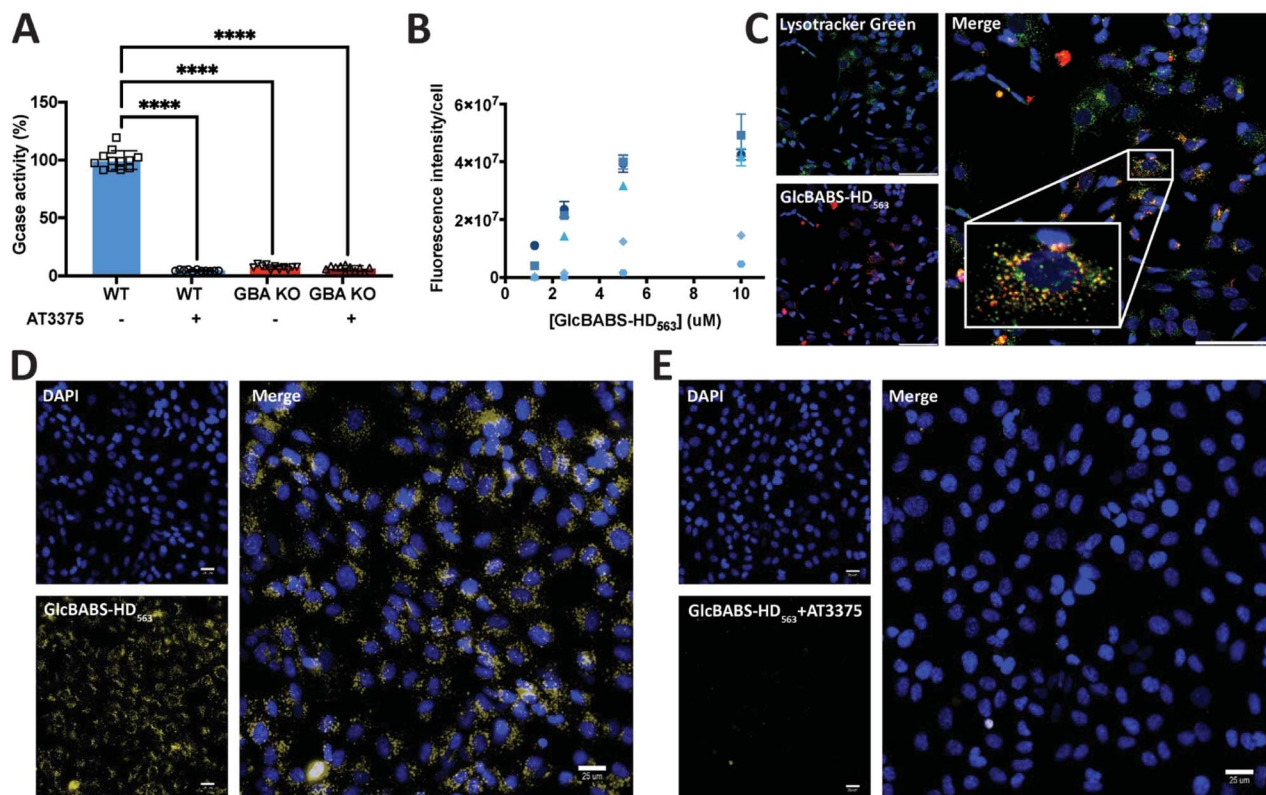


**Fig. 4** GlcBABS-HD<sub>563</sub> is a useful tool to quantitatively measure lysosomal GCase activity in live cells. (A) GlcBABS-HD<sub>563</sub> treated WT cells with/without AT3375 and GBA1 KO with/without AT3375. Significance <0.0001. (B) The signal intensity of GlcBABS-HD<sub>563</sub> within live cells shows a dose and time-dependent response. ● = 0.5 h, ◆ = 1 h, ▲ = 2 h, ■ = 3 h, ● = 4 h. (C) GlcBABS-HD<sub>563</sub> signal intensity is co-localized with LysoTracker™ Green DND-26. (Scale bars represent 80 μm). (D) Image representative of GlcBABS-HD<sub>563</sub> (5 μM for 2 hours) turnover in SK-N-SH cells. (E) Representative image showing that GlcBABS-HD<sub>563</sub> (5 μM for 2 hours) turnover is completely blocked by pre-incubation of SK-N-SH cells with the selective GCase inhibitor AT3375 (10 μM). Nine fields per replicate. ≥ three replicates per condition. Error bars represent the standard error of the mean. (Scale bars represent 25 μm).

measurements of GCase activity. We then investigated the stability of the fluorescent signal arising from GCase catalyzed hydrolysis of GlcBABS-H<sub>563</sub> within live cells. Inadequate stability of the signal arising from enzymatically processed fluorogenic substrates has been previously noted to result not only in poor signal-to-noise but also inaccuracies in measurements due to time dependent signal loss. To address this issue, we used a previously established assay<sup>18</sup> and measured a  $T_{1/2}$  of 64 min for the fluorescent product of GlcBABS-H<sub>563</sub> (Fig. 3B), which is considerably longer than the  $T_{1/2}$  of 19 min observed for the fluorescent products of FQ-GBA and PFB-FDGlu, two other non-lysosomotropic substrates.<sup>18</sup> This greater cellular retention suggests that the aldehyde-tagged fluorophore forms transient imine conjugates as predicted. However, the half-life we observed for GlcBABS-H<sub>563</sub> was much shorter than that observed for LysoFQ-GBA, a lysosomotropic derivative of FQ-GBA, which showed only a 17% decline in signal intensity over 3 hours.<sup>18</sup> Therefore, we considered various alternatives and considered installation of a polylysine moiety as was done for LysoFix-GBA,<sup>5</sup> however, we judged this might be too large in the context of the bis-acetal and felt that a smaller lysosomotropic group should prove adequate to aid retention. We therefore synthesized GlcBABS-HD<sub>563</sub> (Fig. 3A), which includes

the lysosomotropic di-methyllysine (dML) on the proto-aldehyde arm of the bis-acetal motif with the same fluorophore and quencher pair. We then acquired the excitation and emission spectra of GlcBABS-HD<sub>563</sub> (Fig. S3A) and the corresponding products of enzymatic cleavage (Fig. S3B). GlcBABS-HD<sub>563</sub> and the products both exhibited excitation maxima at approximately 540 nm corresponding to the major absorption bands associated with TAMRA. The emission maximum was observed at 565 nm, which is also consistent with the emission bands seen for TAMRA. We next examined GCase catalyzed turnover of GlcBABS-HD<sub>563</sub>. We treated GlcBABS-HD<sub>563</sub> with rhGCase and collected spectral scans at specified intervals over a 150 minutes period (Fig. S3C). We next treated SK-N-SH cells with GlcBABS-HD<sub>563</sub> using the same conditions to compare with GlcBABS-H<sub>563</sub> and found, strikingly, the stability of the fluorescent signal arising from hydrolysis of GlcBABS-HD<sub>563</sub> showed no change over a three-hour time course (Fig. 3C), making this substrate superior to both GlcBABS-H<sub>563</sub> and LysoFQ-GBA.

Encouraged by these results, we next explored whether GlcBABS-HD<sub>563</sub> could usefully quantify GCase activity within the lysosomes of live cells. To do this we used SK-N-SH cells, a neuroblastoma cell line that expresses dopaminergic markers,



as a model system.<sup>19–21</sup> First, we investigated the selectivity of GlcBABS-HD<sub>563</sub> by using both the highly selective GCase inhibitor AT3375 (ref. 22 and 23) and genetic disruption *GBA1* knock-out (KO) SK-N-SH cells.<sup>5</sup> We found that treating cells with AT3375 (10  $\mu$ M) prior to addition of the substrate (5  $\mu$ M) resulted in a complete loss of signal, consistent with our *in vitro* measurements of selectivity. We also found negligible lysosomal GCase activity in *GBA1* KO cells (Fig. 4A, D and E). These data support that GlcBABS-HD<sub>563</sub> is turned over only by GCase within cells. Next, we assessed the dose and time-dependent evolution of the signal within cells to evaluate whether GlcBABS-HD<sub>563</sub> reported on GCase activity in a quantitative manner. These data show linearity in signal intensity over defined ranges, which is necessary for making quantitative measurements of cellular enzymatic activity (Fig. 4B). Finally, we assessed whether GlcBABS-HD<sub>563</sub> reports on the activity of mature GCase, which is found within lysosomes, through colocalization of GCase activity with LysoTracker™ Green DND-26. We observed good spatial correlation, consistent with lysosomal hydrolysis of GlcBABS-HD<sub>563</sub> by lysosomal GCase (Fig. 4C). These collective data support GlcBABS-HD<sub>563</sub> as a tool to quantitatively measure lysosomal GCase activity in live cells.

Having demonstrated that GlcBABS-HD<sub>563</sub> is capable of quantitatively measuring lysosomal GCase activity in live cells, we next turned to our primary goal of investigating whether it could be used to analyze GCase activity within fixed cells. We reasoned that there are two main criteria required of cell active substrates that dictate their utility. First, the fluorescent signal must quantitatively reflect the activities measured within live cells. Second, the distribution of the signal within cells should be retained upon fixation such that spatial information that informs on the subcellular location of the enzyme should be preserved. To solve these problems we were inspired by previous studies that have reported on fluorescence imaging of tissue sections, which have occasionally relied on treatment with sodium borohydride (1%) at low temperature (4 °C) for short periods of time (20 minutes) as a means to reducing

endogenous background fluorescence within tissue samples.<sup>8,24</sup> We expected that borohydride reagents could reduce the possible imine adducts formed from the aldehyde product of GlcBABS-HD<sub>563</sub> with lysosomal proteins to form irreversible secondary amine bioconjugates. Rather than sodium borohydride, we chose the milder and more stable sodium cyanoborohydride (NaCNBH<sub>3</sub>) which is commonly used for reductive amination under aqueous conditions at physiological pH. To approach this problem, we first investigated whether NaCNBH<sub>3</sub> reduction would lead to stable fluorescent protein-labelling following turnover of GlcBABS-HD<sub>563</sub>. To test this possibility, we treated GlcBABS-HD<sub>563</sub> (5  $\mu$ M) for two hours with rhGCase in the presence of bovine serum albumin (BSA), after which we added NaCNBH<sub>3</sub> or buffer alone. The reaction was then terminated by mixing with Laemmli buffer containing reducing agents and the proteins were then resolved by polyacrylamide gel electrophoresis (PAGE). The resulting gel was stained and then imaged to record both total protein (Coomassie) and TAMRA-conjugated proteins (fluorescence). BSA-TAMRA and GCase-TAMRA conjugates were only observed in samples containing GCase that were treated with NaCNBH<sub>3</sub> (Fig. 5A and B). Moreover, inhibition of GCase prevented any labelling. These data show that the aldehyde product arising from turnover of GlcBABS-HD<sub>563</sub> can form imine conjugates with proteins that can in turn be reduced to form stable adducts. In addition, we evaluated the *in vitro* stability of TAMRA in the presence of different concentrations of NaCNBH<sub>3</sub> and found, as expected, no significant change in fluorescent intensity (Fig. S4).

To determine the optimal methods for reduction of imine adducts within cells in a manner that was compatible with standard fixation methods, we treated SK-N-SH cells with 5  $\mu$ M GlcBABS-HD<sub>563</sub> for two hours, and subsequently fixed cells using standard PFA conditions involving 4% PFA solution at 20 °C for 30 minutes.<sup>25</sup> We followed this up by treatment with different concentrations of NaCNBH<sub>3</sub> and different incubation times. We found that the fluorescence intensity depends on the concentration of NaCNBH<sub>3</sub>, with the optimized conditions

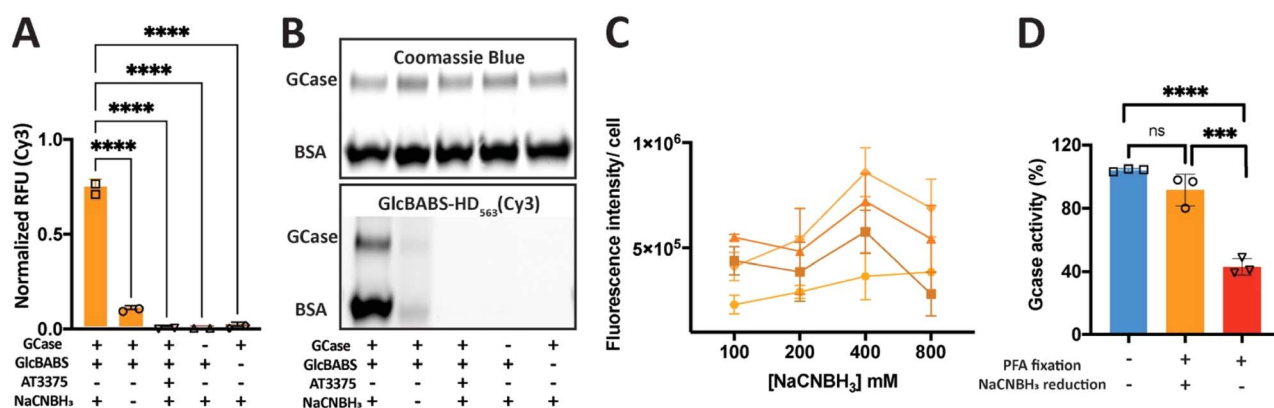
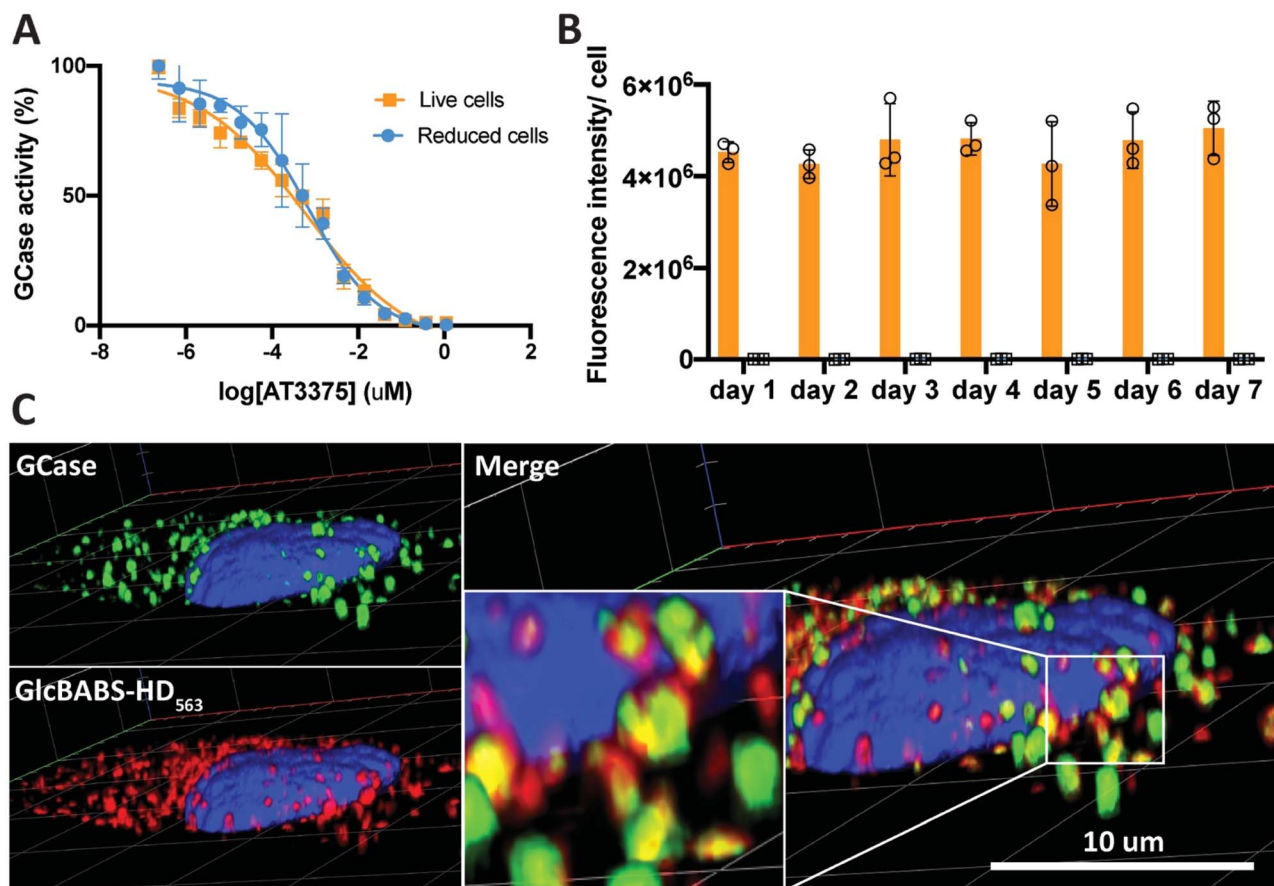


Fig. 5 In-gel and in-cell validation and imine reduction optimization in cells. (A) Quantification of signal intensity from imaging, signals are normalized to protein levels. Significance <0.0001. (B) NaCNBH<sub>3</sub> treatment maintained the fluorescent signal on proteins whereas the non-NaCNBH<sub>3</sub> treatment showed little fluorescence. (C) Optimization of NaCNBH<sub>3</sub> treatment conditions. ● = 0 h, ◆ = 1 h, ▲ = 3 h, ■ = 24 h. (D) Comparison with/without NaCNBH<sub>3</sub> treatment in a cell assay, fluorescent signals are shown for live cells (blue), fixed cells with NaCNBH<sub>3</sub> treatment (orange), and fixed cells without NaCNBH<sub>3</sub> treatment (red). Significance <0.0001. Error bars represent the standard error of the mean (*n* = 3). For the uncropped images see Fig. S6.



**Fig. 6** Quantitative measurement in live and reduced cells and co-localization with anti-GCase antibody. (A) Comparison of the IC<sub>50</sub> curves for the selective GCase inhibitor AT3375 measured using GlcBABS-HD<sub>563</sub> in live (orange) and reduced (blue) cells. (Error bars represent standard deviation,  $n = 3$ , nine fields per replicate). (B) GlcBABS-HD<sub>563</sub> fluorescent signal is stable after imine reduction over a week, non-inhibition in orange, AT3375 inhibition in blue. (No significance, error bars represent standard deviation,  $n = 3$ , nine fields per replicate). (C) Confocal images show a high degree of co-localization of GCase activity (red) and GCase protein (green) within fixed SK-N-SH cells.

being found to be 400 mM NaCNBH<sub>3</sub> with a 1-hour incubation time (Fig. 5C). These conditions are similar to previous reports on the reduction of cell surface imine adducts with NaCNBH<sub>3</sub>.<sup>26</sup> Importantly, we found that the fluorescent signals retained their punctate distribution (Fig. S5), suggesting that this method leads to retention of the adducts within lysosomes. Excluding NaCNBH<sub>3</sub> treatment led to a striking 85% decrease in fluorescence intensity (Fig. 5D). These collective data show that simple reductive amination, in conjunction with PFA fixation, leads to GCase-dependent formation of stable fluorescent adducts that do not diffuse throughout the cell. Thus, GlcBABS-HD<sub>563</sub> should be well suited to quantify lysosomal GCase activity while enabling immunocytochemical (ICC) study of cellular proteins.

We next turned to our primary goal of investigating whether it could be used to quantify lysosomal GCase activity within fixed cells. We reasoned there are two main criteria required of fixable fluorescence quenched substrates that dictate their utility. First, the fluorescent signal must quantitatively reflect the activities measured within live cells. Second, the distribution of the signal within cells should be preserved. To assess the quantitative performance of GlcBABS-HD<sub>563</sub> in fixed cells we determined the cellular IC<sub>50</sub> of AT3375 in live cells and then

treated the cells with a reductant and fixed them before imaging and analysis. Using this approach, we measured a cellular IC<sub>50</sub> value of  $6 \pm 3$  nM in live cells and a closely similar value of  $7 \pm 3$  nM in fixed cells (Fig. 6A). These data demonstrated that the quantitative measurements made in live cells are preserved upon NaCNBH<sub>3</sub> reduction and cellular fixation. Notably, we also observed that the signal was stable over seven days, which is consistent with the fluorescent product being covalently linked to proteins (Fig. 6B). Analysis of co-localization of the product of GlcBABS-HD<sub>563</sub> and GCase protein showed excellent overlap (PCC = 0.74, Fig. 6C), which was in agreement with the live cell colocalization using LysoTracker™ Green-DND26. These data together show that GlcBABS-HD<sub>563</sub> reports quantitatively on lysosomal GCase activity in both live and fixed cells.

## Conclusion

The ability of fluorescence-quenched substrates to provide quantitative and spatial information on the function of target enzymes makes them valuable tools for understanding fundamental cellular biochemistry. One common shortcoming associated with these substrates is their inability to simultaneously quantify enzyme activity and perform other biochemical





measurements, complicating mechanistic studies on the regulation of enzymes within cells. This challenge is exemplified by the difficulty of studying GCase activity in live cells and, in turn, understanding the underlying factors that influence its activity.<sup>27,28</sup> Here we describe GlcBABS-HD<sub>563</sub>, a fluorescence quenched substrate, and detailed methods that allow this substrate to be used to quantitatively report on the intracellular levels of GCase activity in both live and fixed cells. Importantly, we show that quantitative measurements made in live cells correlate with those made in fixed cells and that the resulting signal is stable upon fixation for at least seven days. The ability to quantify GCase activity within stably fixed cells should make this substrate more widely useful to the community since it does not necessitate rapid manipulation of microplates and timely image-based analyses. Moreover, fixation of samples should enable higher throughput experiments, including screening to identify small molecule modifiers of GCase activity, which would be technically demanding to perform in live cells.<sup>29</sup> Finally, we demonstrate that GlcBABS-HD<sub>563</sub> can be used in conjunction with immunocytochemistry (ICC). We anticipate that such concomitant measurements could provide new insights into the function of known regulatory proteins such as Saposin C or lysosomal integral membrane protein-2 (LIMP-2). Using this substrate, it will be readily feasible to perform co-localization of such proteins alongside both GCase protein and activity in a cell-by-cell manner. Regardless, previous studies have relied on the analysis of parallel samples using techniques such as immunoblotting, which do not report on either the subcellular distribution of GCase activity or its lysosomal levels. Finally, the modular design of GlcBABS-HD<sub>563</sub>, coupled with the late-stage installation of chromophores, should enable the generation of substrates having various excitation and emission properties as well as ratiometric substrates.<sup>30</sup> Because LysoFix-GBA has multiple primary amine functionalities, fixation with PFA leads to fixation of both the substrate and product. In contrast, the proto-aldehyde of GlcBABS-HD<sub>563</sub> is only revealed following enzymatic hydrolysis but requires a reduction step. Drawing direct comparisons between these two chemistries is therefore somewhat difficult, however, which one provide superior performance may depend on the specific case. However, we note that the stability of the product of GlcBABS-HD<sub>563</sub>, when fixed in cells, exceeds that observed for LysoFix-GBA.<sup>5</sup> The basis for this difference likely stems from the different chemistry used in fixation, where the reduction step leads to a highly stable secondary amine crosslink. In any event, we anticipate that GlcBABS-HD<sub>563</sub> will open the door to new experiments to study the regulation of GCase activity within living cells. Finally, because the BABS concept does not require modification of the substrate recognition group, unlike other recently described live cell GCase substrates,<sup>5,18,30</sup> we expect that application of this strategy to other hydrolytic enzymes should be quite feasible.

## Author contributions

SZ; conceptualization, methodology, investigation, resources, validation, data curation, writing – original draft, writing – review and editing, formal analysis, supervision. MCD; conceptualization, methodology, investigation, data curation,

resources, writing – original draft, writing – review and editing, formal analysis. SC; resources, investigation, data curation, writing – review and editing. K LW; investigation, validation, data curation, writing – review and editing. EPR; resources, investigation, data curation, writing – review and editing. WBW; investigation, data curation, writing – review and editing. DJV; conceptualization, funding acquisition, project administration, writing – original draft, writing – review and editing, formal Analysis, supervision.

## Conflicts of interest

The substrates described are the subject of a patent application held by Simon Fraser University, with several of the authors listed as inventors.

## Data availability

Raw imaging data are available from the authors on reasonable request.

Supplementary information: the experimental section, figures and tables; NMR spectra; and other details. See DOI: <https://doi.org/10.1039/d5sc04671h>.

## Acknowledgements

The authors are grateful for support from the Natural Sciences and Engineering Research Council (NSERC) of Canada (RGPIN-05426) and the Canadian Glycomics Network (RG-1). D. J. V. acknowledges the Canada Research Chairs program for support as a Tier I Canada Research Chair in Chemical Biology. M. C. D. was supported by a NSERC PGS-D scholarship. S. C. thanks the Canadian Institutes of Health Research (CIHR) for a post-doctoral fellowship, and S. C. is now supported by NSERC (RGPIN-2019-05451) and by the Fonds de Recherche du Québec – Nature et Technologies (2021-NC281486). The authors also thank Gideon Davies for providing the sample of the GBA2 enzyme and the Centre for High-Throughput Chemical Biology (HTCB) for access to core facilities.

## References

- W. Chyan and R. T. Raines, *ACS Chem. Biol.*, 2018, **13**, 1810–1823.
- K. M. T. H. Rahit and M. Tarailo-Graovac, *Genes*, 2020, **11**, 239.
- S. Li, L. Wang, F. Yu, Z. Zhu, D. Shobaki, H. Chen, M. Wang, J. Wang, G. Qin, U. J. Erasquin, L. Ren, Y. Wang and C. Cai, *Chem. Sci.*, 2017, **8**, 2107–2114.
- T. Walter, L. Collenburg, L. Japtok, B. Kleuser, S. Schneider-Schaulies, N. Müller, J. Becam, A. Schubert-Unkmeir, J. N. Kong, E. Bieberich and J. Seibel, *Chem. Commun.*, 2016, **52**, 8612–8614.
- S. Zhu, M. C. Deen, Y. Zhu, P.-A. Gilormini, X. Chen, O. B. Davis, M. Y. Chin, A. G. Henry and D. J. Vocadlo, *Angew. Chem., Int. Ed.*, 2023, **62**, e202309306.





- 6 S. Cecioni and D. J. Voadlo, *J. Am. Chem. Soc.*, 2017, **139**, 8392–8395.
- 7 S. Cecioni, R. A. Ashmus, P.-A. Gilormini, S. Zhu, X. Chen, X. Shan, C. Gros, M. C. Deen, Y. Wang, R. Britton and D. J. Voadlo, *Nat. Chem. Biol.*, 2022, **18**, 332–341.
- 8 B. Clancy and L. J. Cauller, *J. Math. Neurosci.*, 1998, **83**, 97–102.
- 9 D. E. C. Boer, J. van Smeden, J. A. Bouwstra and J. M. F. G. Aerts, *J. Clin. Med.*, 2020, **9**, 736.
- 10 R. O. Brady, J. N. Kanfer and D. Shapiro, *Biochem. Biophys. Res. Commun.*, 1965, **18**, 221–225.
- 11 G. M. Riboldi and A. B. Di Fonzo, *Cells*, 2019, **8**, 364.
- 12 S. Jesús, I. Huertas, I. Bernal-Bernal, M. Bonilla-Toribio, M. T. Cáceres-Redondo, L. Vargas-González, M. Gómez-Llamas, F. Carrillo, E. Calderón, M. Carballo, P. Gómez-Garre and P. Mir, *PLoS One*, 2016, **11**, e0167749.
- 13 C. Blauwendraat, X. Reed, L. Krohn, K. Heilbron, S. Bandres-Ciga, M. Tan, J. R. Gibbs, D. G. Hernandez, R. Kumaran, R. Langston, L. Bonet-Ponce, R. N. Alcalay, S. Hassin-Baer, L. Greenbaum, H. Iwaki, H. L. Leonard, F. P. Grenn, J. A. Ruskey, M. Sabir, S. Ahmed, M. B. Makarious, L. Pihlstrøm, M. Toft, J. J. van Hilten, J. Marinus, C. Schulte, K. Brockmann, M. Sharma, A. Siitonen, K. Majamaa, J. Eerola-Rautio, P. J. Tienari, A. Pantelyat, A. E. Hillis, T. M. Dawson, L. S. Rosenthal, M. S. Albert, S. M. Resnick, L. Ferrucci, C. M. Morris, O. Pletnikova, J. Troncoso, D. Grosset, S. Lesage, J.-C. Corvol, A. Brice, A. J. Noyce, E. Masliah, N. Wood, J. Hardy, L. M. Shulman, J. Jankovic, J. M. Shulman, P. Heutink, T. Gasser, P. Cannon, S. W. Scholz, H. Morris, M. R. Cookson, M. A. Nalls and Z. Gan-Or, AB Singleton, and on behalf of the International Parkinson's Disease Genomics Consortium (IPDGC), *Brain*, 2020, **143**, 234–248.
- 14 Z. Gan-Or, I. Amshalom, A. Bar-Shira, M. Gana-Weisz, A. Mirelman, K. Marder, S. Bressman, N. Giladi and A. Orr-Urtreger, *J. Neurol.*, 2015, **262**, 2443–2447.
- 15 D. S. Larsen, A. Schofield, R. J. Stoodley and P. D. Tiffin, *J. Chem. Soc., Perkin Trans. 1*, 1996, 2487–2495.
- 16 A. K. Yadav, D. L. Shen, X. Shan, X. He, A. R. Kermode and D. J. Voadlo, *J. Am. Chem. Soc.*, 2015, **137**, 1181–1189.
- 17 M. S. Idris, D. S. Larsen, R. G. Pritchard, A. Schofield, R. J. Stoodley and P. D. Tiffin, *J. Chem. Soc., Perkin Trans. 1*, 2000, 2195–2204.
- 18 M. C. Deen, Y. Zhu, C. Gros, N. Na, P.-A. Gilormini, D. L. Shen, S. Bhosale, N. Anastasi, R. Wang, X. Shan, E. Harde, R. Jagasia, F. C. Lynn and D. J. Voadlo, *Proc. Natl. Acad. Sci. U. S. A.*, 2022, **119**, e2200553119.
- 19 C. Fernández-Moriano, E. González-Burgos and M. P. Gómez-Serranillos, *Oxid. Med. Cell. Longev.*, 2015, **2015**, 408927.
- 20 W. S. Kim and G. M. Halliday, *J. Parkinsons Dis.*, 2012, **2**, 41–46.
- 21 X. Du, H. Xu, L. Shi, Z. Jiang, N. Song, H. Jiang and J. Xie, *Sci. Rep.*, 2016, **6**, 33674.
- 22 M. C. Deen, C. Proceviat, X. Shan, L. Wu, D. L. Shen, G. J. Davies and D. J. Voadlo, *ACS Chem. Biol.*, 2020, **15**, 824–829.
- 23 J. Gordon, S. Amini and M. K. White, in *Neuronal Cell Culture: Methods and Protocols*, ed. S. Amini and M. K. White, Humana Press, Totowa, NJ, 2013, pp. 1–8.
- 24 P. Tagliaferro, C. J. Tandler, A. J. Ramos, J. Pecci Saavedra and A. Brusco, *J. Math. Neurosci.*, 1997, **77**, 191–197.
- 25 D. Hopwood, *Histochem. J.*, 1985, **17**, 389–442.
- 26 X. M. Gao and J. Rhodes, *J. Immunol.*, 1990, **144**, 2883–2890.
- 27 J.-R. Alattia, J. E. Shaw, C. M. Yip and G. G. Privé, *Proc. Natl. Acad. Sci. U. S. A.*, 2007, **104**, 17394–17399.
- 28 A. Velayati, J. DePaolo, N. Gupta, J. H. Choi, N. Moaven, W. Westbroek, O. Goker-Alpan, E. Goldin, B. K. Stubblefield, E. Kolodny, N. Tayebi and E. Sidransky, *Hum. Mut.*, 2011, **32**, 1232–1238.
- 29 D. Williams, L. M. Glasstetter, T. T. Jong, T. Chen, A. Kapoor, S. Zhu, Y. Zhu, R. Calvo, A. Gehrlein, K. Wong, A. N. Hogan, D. J. Voadlo, R. Jagasia, J. J. Marugan, E. Sidransky, M. J. Henderson and Y. Chen, *Proc. Natl. Acad. Sci. U. S. A.*, 2024, **121**, e2406009121.
- 30 B. Tiet, S. Zhu, X. Chen, N. Anastasi, N. W. See, M. C. Deen, E. Harde and D. J. Voadlo, *RSC Chem. Biol.*, 2025, **6**, 1297–1305.

